

Electronic Supplementary Information

for

Direct *in situ* measurement of polymorphic transition temperatures under thermo-mechanochemical conditions

Jasna Alić,^{*a} Ivor Lončarić,^a Martin Etter,^b Mirta Rubčić,^c Zoran Štefanić,^a Marina Šekutor,^{*a} Krunoslav Užarević^{*a} and Tomislav Stolar^{*a†}

^a Ruđer Bošković Institute, Bijenička c. 54, 10000 Zagreb, Croatia.

^b Deutsches Elektronen-Synchrotron (DESY), Notkestraße 85, 22607 Hamburg, Germany.

^c Department of Chemistry, Faculty of Science, University of Zagreb, Horvatovac 102a, 10000 Zagreb, Croatia.

† Current address: Federal Institute for Materials Research and Testing (BAM), 12489 Berlin, Germany.

E-mail: jasna.alic@irb.hr; marina.sekutor@irb.hr; krunoslav.uzarevic@irb.hr;
tomislav.stolar@gmail.com

General

1-adamantyl-1-diamantyl ether was synthesized by high-temperature ball milling according to the published procedure.¹ GC-MS analyses were performed on an Agilent 7890B/5977B GC/MSD instrument equipped with a HP-5ms column. Laboratory ball milling experiments were conducted with IST 500 vibratory ball mill using 10 mL Teflon jars placed inside a larger aluminum container. Thermo-mechanochemical reactions were conducted with an external 75W band heater and a proportional–integral–derivative controller according to a previously published procedure.² Programmable heating regimes were enabled by OMEGA Platinum controller equipped with a ramp heating option.³ To ensure the most precise reading of the reaction mixture temperature and prevent underheating of the reaction mixture due to the thermal inertia of the PTFE insert, we used a TME K-type thermocouple with a 0.8 diameter mm head embedded in the PTFE insert at a distance of less than one mm from the interior wall of the insert. The time resolution for the temperature logging was 1 second.

All milling reactions were conducted by milling 200 mg of 1-adamantyl-1-diamantyl ether at 30 Hz frequency using two 7 mm stainless steel (SS) balls as a grinding media. LAG experiments were conducted with 46 μL of liquid additives ($\eta = 0.23 \mu\text{L}/\text{mg}$). ^{13}C and ^1H solid-state NMR measurements were recorded on a 600 MHz Varian NMR spectrometer (Varian, Palo Alto, CA, USA) using 1.6 mm HXYMAS probe. Samples were spun at 20 kHz. The ^1H – ^{13}C cross-polarization magic-angles pinning (CP–MAS) experiments consisted of the proton $\pi/2$ pulse with a pulse length of 2.3 and 2.1 μs for the polymorph α and β , respectively and a ramped-amplitude (RAMP) CP block of 4.0 ms. The numbers of scans for the ^1H – ^{13}C CP-MAS were 2300 and 16000 and a repetition delay of 30 and 5 s was used for the polymorph α and β , respectively. The ^{13}C and ^1H Larmor frequencies were 150.72 MHz and 599.33 MHz, respectively. The obtained spectra were calibrated according to the ^{13}C signals of the tetramethyl silane. PXRD patterns were collected on a PanAlytical Aeris diffractometer (Cu $K\alpha$ radiation and Ni filter) in Bragg-Brentano geometry using zero background sample holder. Variable-temperature PXRD patterns were collected using a TTK 400 Anton Paar thermal camera on PanAlytical Aeris diffractometer ($\lambda = 1.54175 \text{ \AA}$) on a zero background sample holder. After reaching the desired temperature setpoint, the sample was thermally equilibrated for 1 min after which the diffraction data were collected with the collection program time of 30 min. *In situ* monitoring of thermo-mechanochemical reactions was performed by synchrotron powder X-ray diffraction at the P02.1 beamline at PETRA III, DESY (Hamburg, Germany). For *in situ* monitoring, ball milling was conducted with IST-636 mixer mill (InSolido Technologies, Croatia, Zagreb). The X-ray beam ($\lambda = 0.20741 \text{ \AA}$) was set to pass through the Teflon reaction vessel. Exposure time was set to 10 s. Diffraction data were collected on a Perkin Elmer XRD1621 flat-panel detector positioned 1595 mm from the sample, which consisted of an amorphous Si sensor equipped with a CsI scintillator (pixel number: 2048 x 2048, pixel size: 200x200 μm^2). To obtain the classic one-dimensional PXRD pattern, the two-dimensional diffraction images were integrated with the DAWN Science package. 2D time-resolved plots of *in situ* monitoring data were created in MATLAB and the background of each diffraction pattern was subtracted prior to plotting using the Sonneveld-Visser algorithm.⁴ Differential scanning calorimetry (DSC) analysis was performed with a TA DSC 25 calorimeter using standard aluminum pans. Between 1.0 mg and 2.0 mg of sample were used. All experiments were conducted in a dynamic nitrogen atmosphere with a flow rate of 50 $\text{cm}^3 \text{ min}^{-1}$ and with heating rate of 5 and 10 K min^{-1} .

Crystallography

Single crystals of polymorph β were grown by recrystallising 1-adamantyl-1-diamantyl ether sample that heated to 115 $^\circ\text{C}$ in THF. Single crystal measurements were performed on XtaLAB Synergy, Dualflex, HyPix (micro-focus sealed X-ray tube). Using Olex2,⁵ the structures were

solved with the ShelXT⁶ structure solution program using Intrinsic Phasing and refined with the ShelXL refinement package using Least Squares minimization. Hydrogen atoms in these structures were introduced at calculated positions and treated using appropriate riding models; all non-hydrogen atoms were refined anisotropically. The crystal structure of polymorph β reported herein was deposited in the CSD and was allocated the 2270174 CCDC deposition number. The data can be obtained free of charge from the CCDC via www.ccdc.cam.ac.uk/data_request/cif.

Table S1. Crystallographic, data collection and refinement data for single crystal X-ray diffraction.

Compound	polymorph β
Empirical formula	C ₂₄ H ₃₄ O
Formula wt. / g mol ⁻¹	338.51
Colour	colourless
Crystal dimensions / mm	0.40 x 0.20 x 0.20
Space group	
<i>a</i> / Å	7.7886(5)
<i>b</i> / Å	10.8558(5)
<i>c</i> / Å	11.3845(4)
α / °	76.757(4)
β / °	84.981(4)
γ / °	78.050(5)
<i>Z</i>	2
<i>V</i> / Å ³	915.86(8)
<i>D</i> _{calc} / g cm ⁻³	1.227
λ / Å	1.54184 (CuK α)
μ / mm ⁻¹	0.542
Θ range / °	5.0110 – 78.7960
<i>T</i> / K	296.69(13)
Diffractometer type	XtaLAB Synergy
	-9 < <i>h</i> < 9;
Range of <i>h</i> , <i>k</i> , <i>l</i>	-13 < <i>k</i> < 13;
	-14 < <i>l</i> < 11

Reflections collected	11118
Independent reflections	3740
Observed reflections ($I \geq 2\sigma$)	3029
Absorption correction	Multi-scan
T_{\min} , T_{\max}	0.75624; 1.0000
R_{int}	0.0672
$R(F)$	0.0914
$R_w(F^2)$	0.3245
Goodness of fit	1.428
H atom treatment	Constrained
No. of parameters	226
No. of restraints	0
$\Delta\rho_{\max}$, $\Delta\rho_{\min}$ ($e\text{\AA}^{-3}$)	0.634; -0.538

Computation

All density functional theory (DFT) calculations have been performed with PBE⁷+MBD⁸ exchange-correlation functional using an intermediate basis set as implemented in FHI-aims code, version 221103.1.^{9,10} The experimental structure was relaxed until the forces on all atoms were lower than 0.01 eV/Å. For free energy calculations, we used ANI-2x¹¹ machine learning interatomic potential, as implemented in TorchANI.¹² We have added D4¹³ dispersion correction on top of the ANI-2x, for the final Atomic Simulation Environment¹⁴ (ASE) calculator. Helmholtz free energy was calculated in harmonic approximation from finite difference phonons with each supercell axis of at least 13 Å, as implemented in phonopy.^{15,16}

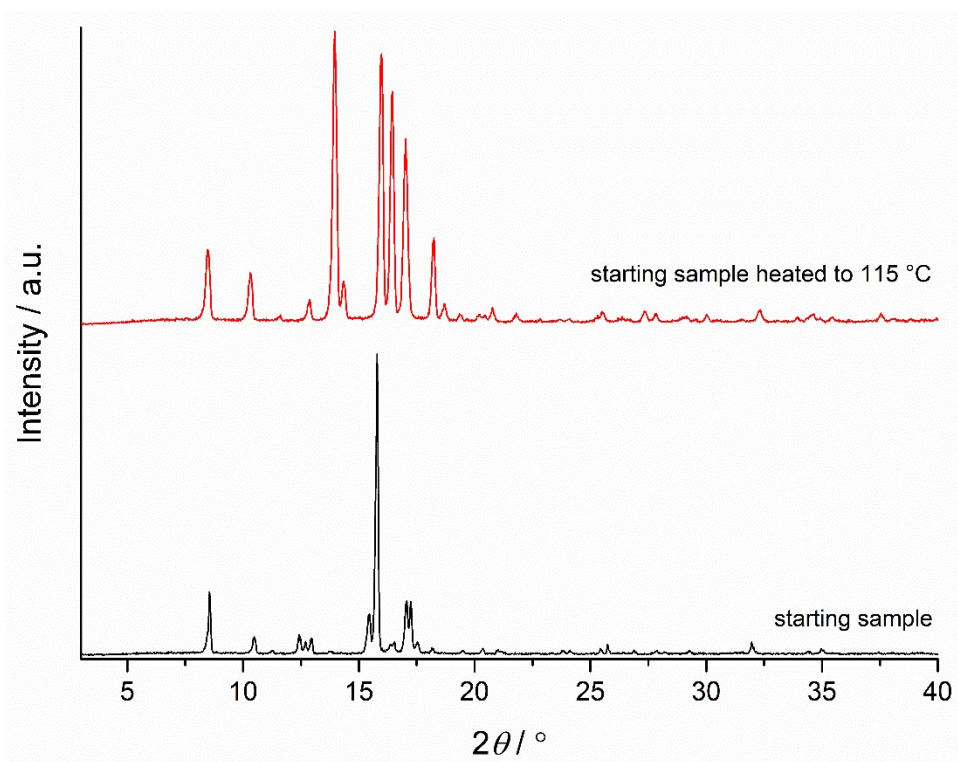


Fig. S1. PXRD patterns showing the formation of new crystalline phase after heating the starting 1-adamantyl-1-diamantyl ether to 115 °C in a DSC experiment ($\lambda = 1.54 \text{ \AA}$).

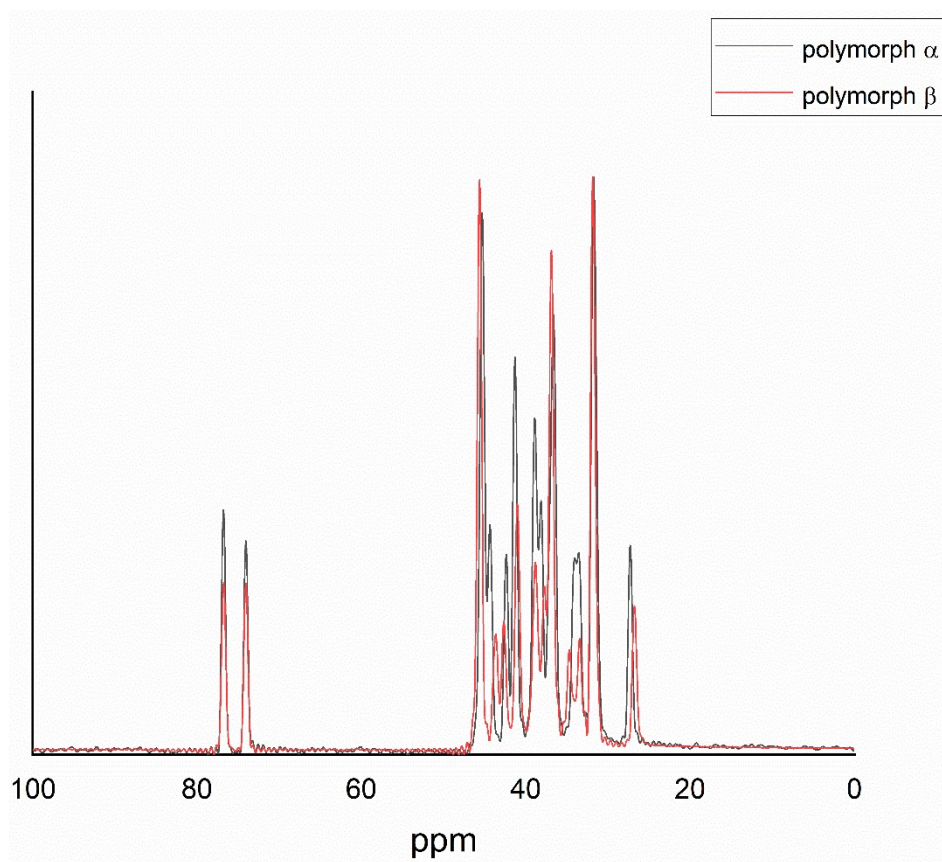


Fig. S2. ^1H - ^{13}C cross-polarization magic-angle spinning (CPMAS) nuclear magnetic resonance spectra of polymorphs α and β .

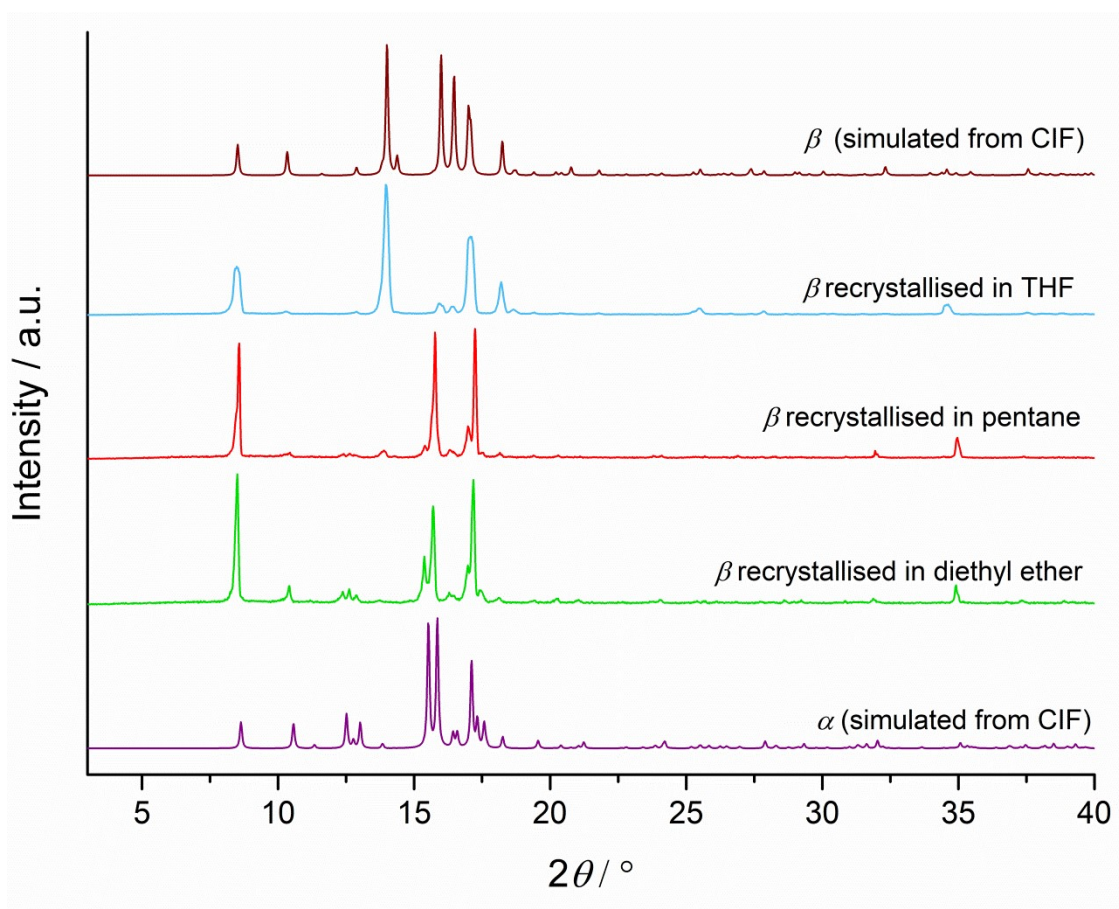


Fig. S3. PXRD patterns showing the results of recrystallisation experiments ($\lambda = 1.54 \text{ \AA}$).

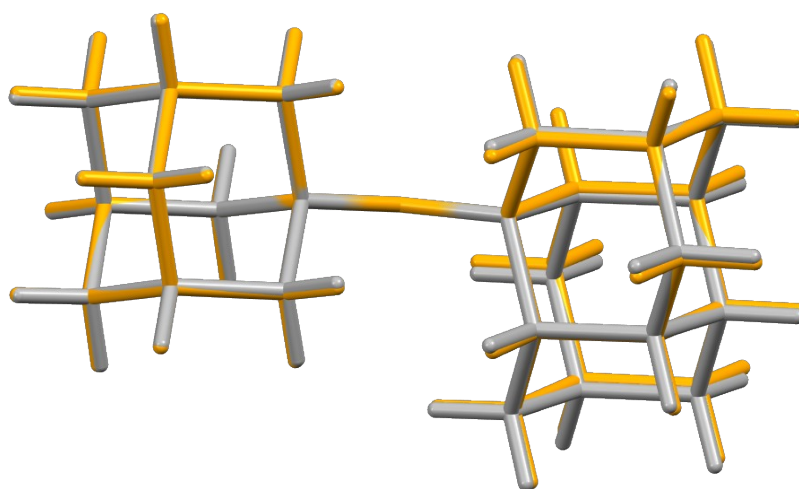


Fig. S4. Overlay of the molecular structures present in polymorph alpha (orange) and polymorph beta (grey). Molecules were overlapped through the central C–O–C linkage.

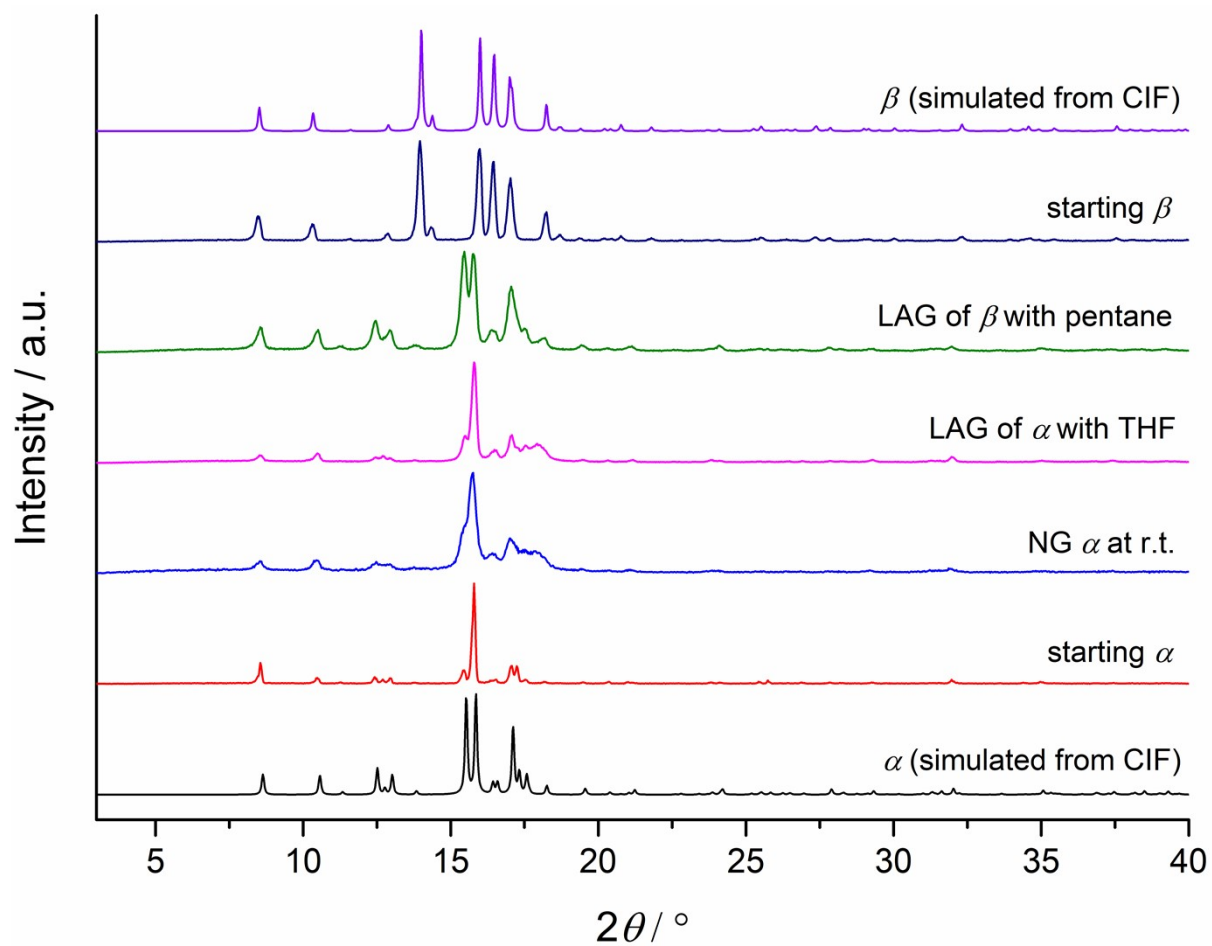


Fig. S5. PXRD patterns showing the results of milling polymorphs α and β under different conditions at room temperature ($\lambda = 1.54 \text{ \AA}$).

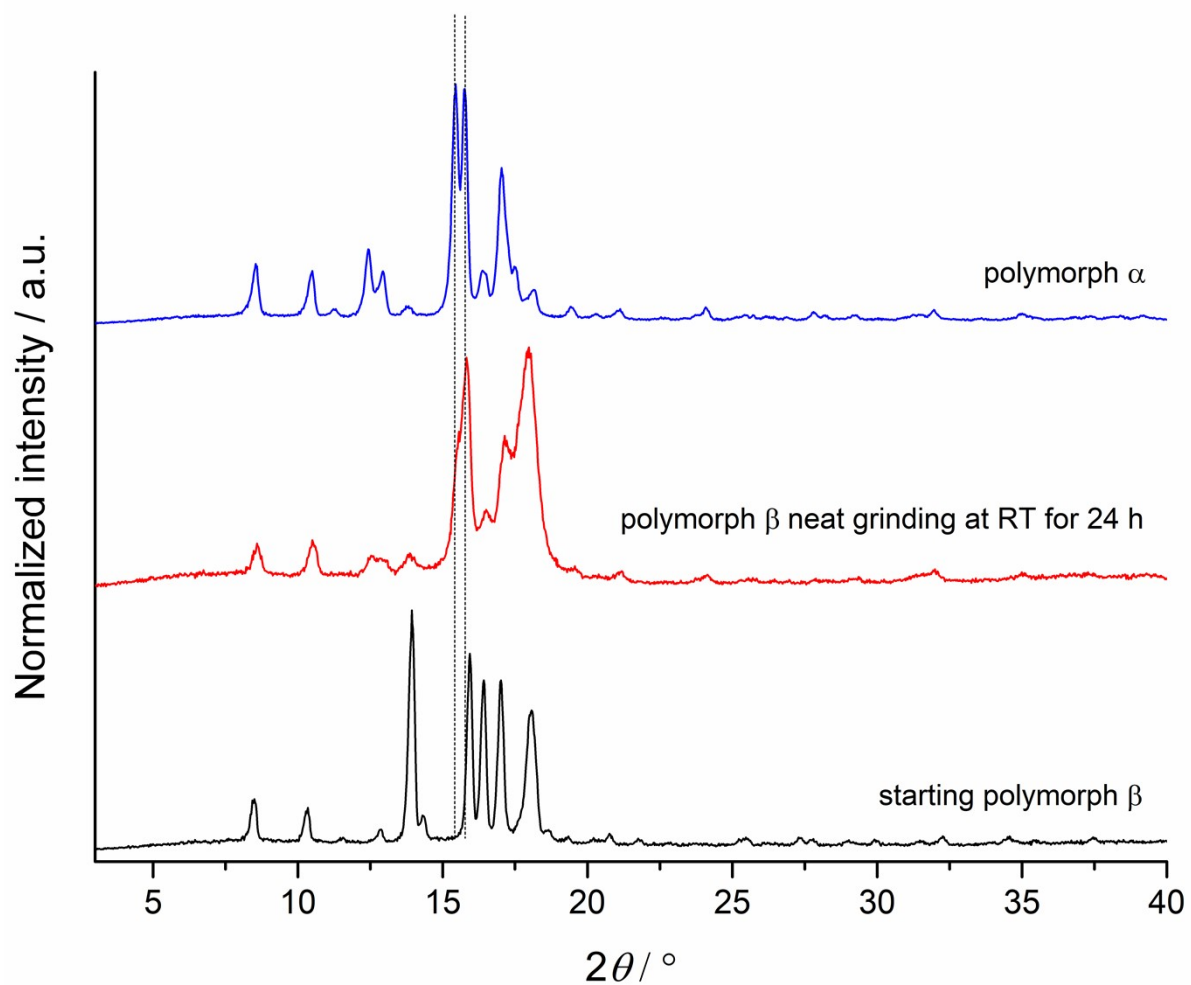


Fig. S6. PXRD patterns showing that polymorph β started to transform to polymorph α after neat grinding at room temperature for 24 h ($\lambda = 1.54 \text{ \AA}$). Polymorphic transformation was not complete and a mixture of polymorphs was obtained.



Fig. S7. Front view of our thermo-mechanochemical reaction setup at DESY synchrotron. Jar size is 8 cm in length.

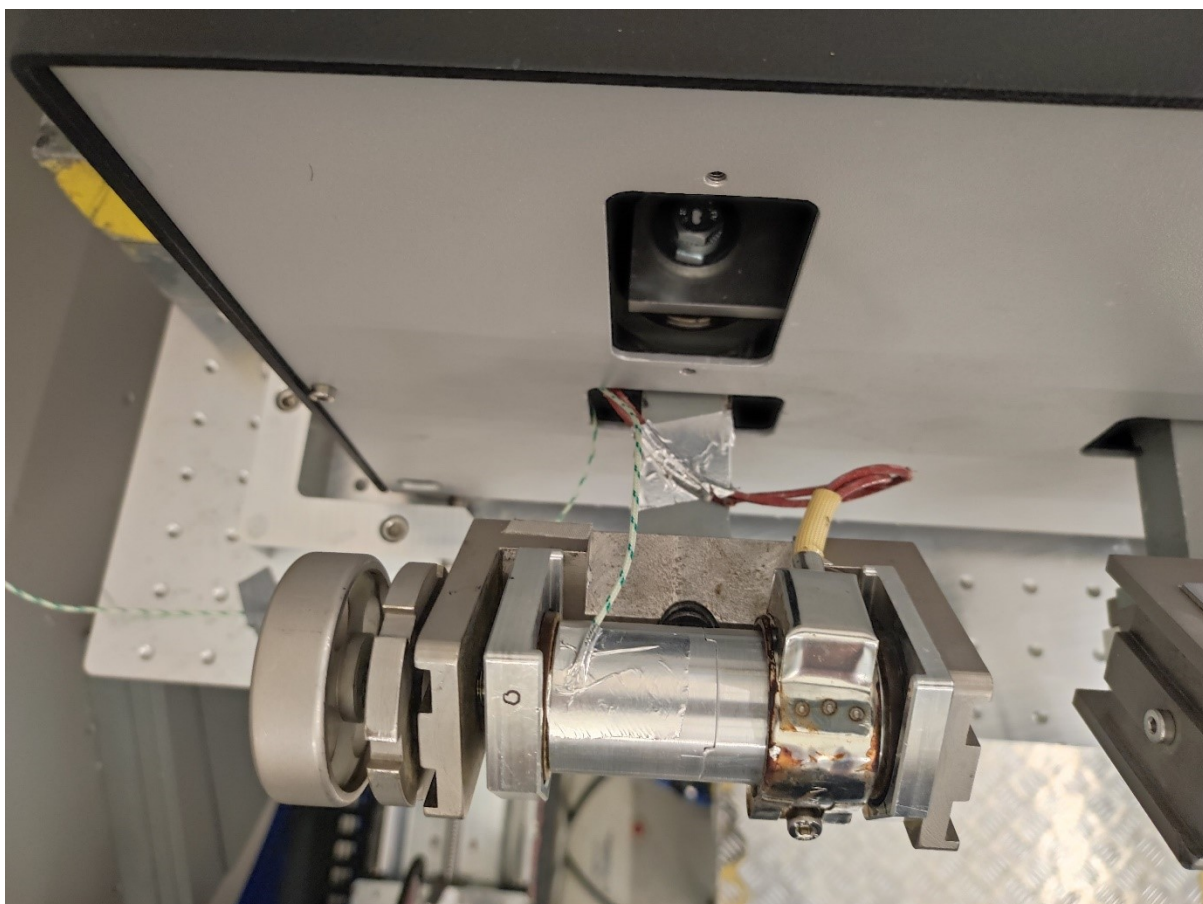


Fig. S8. Top view of our thermo-mechanochemical reaction setup at DESY synchrotron. Jar size is 8 cm in length.

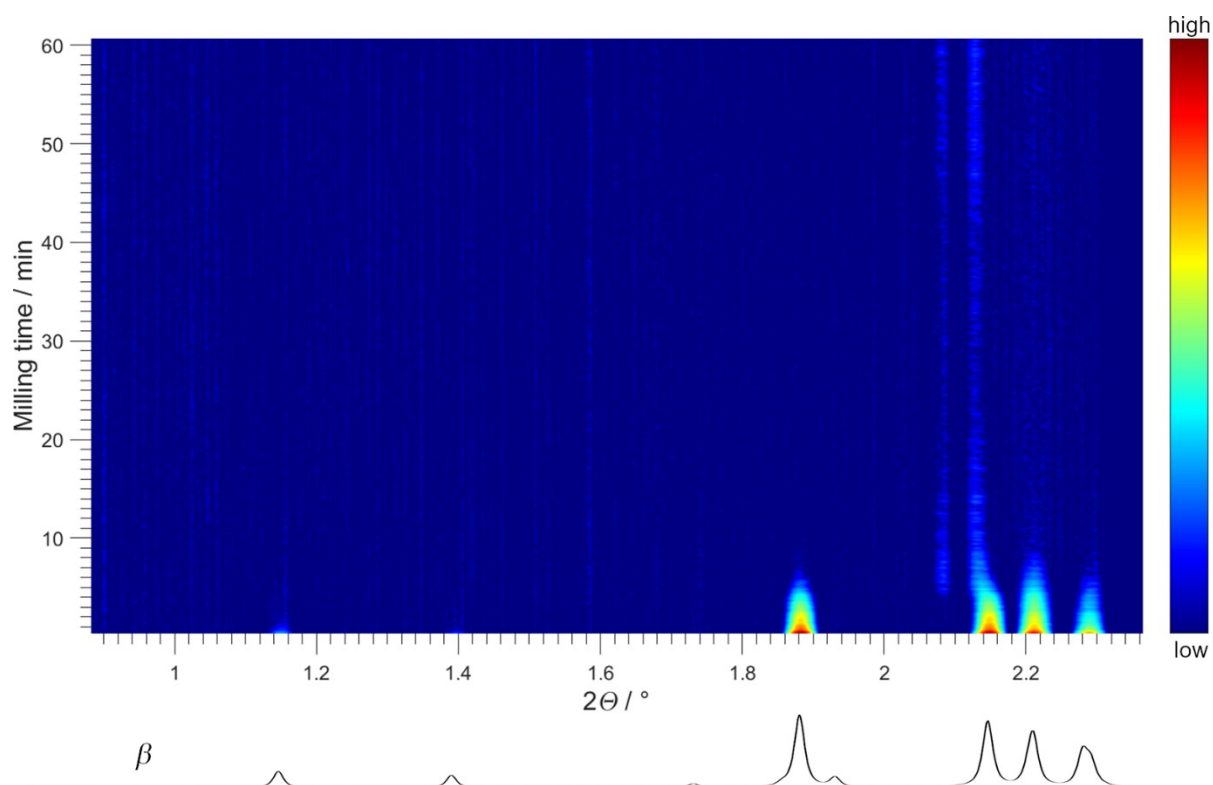


Fig. S9. In situ monitoring of LAG polymorph β with pentane by synchrotron PXRD ($\lambda = 0.20741 \text{ \AA}$). Disappearance of diffraction peaks after ca. 6 min of milling time was attributed to the change in rheology of the reaction mixture and inhomogeneous distribution of the milled sample, which led to its disappearance from the X-ray beam.

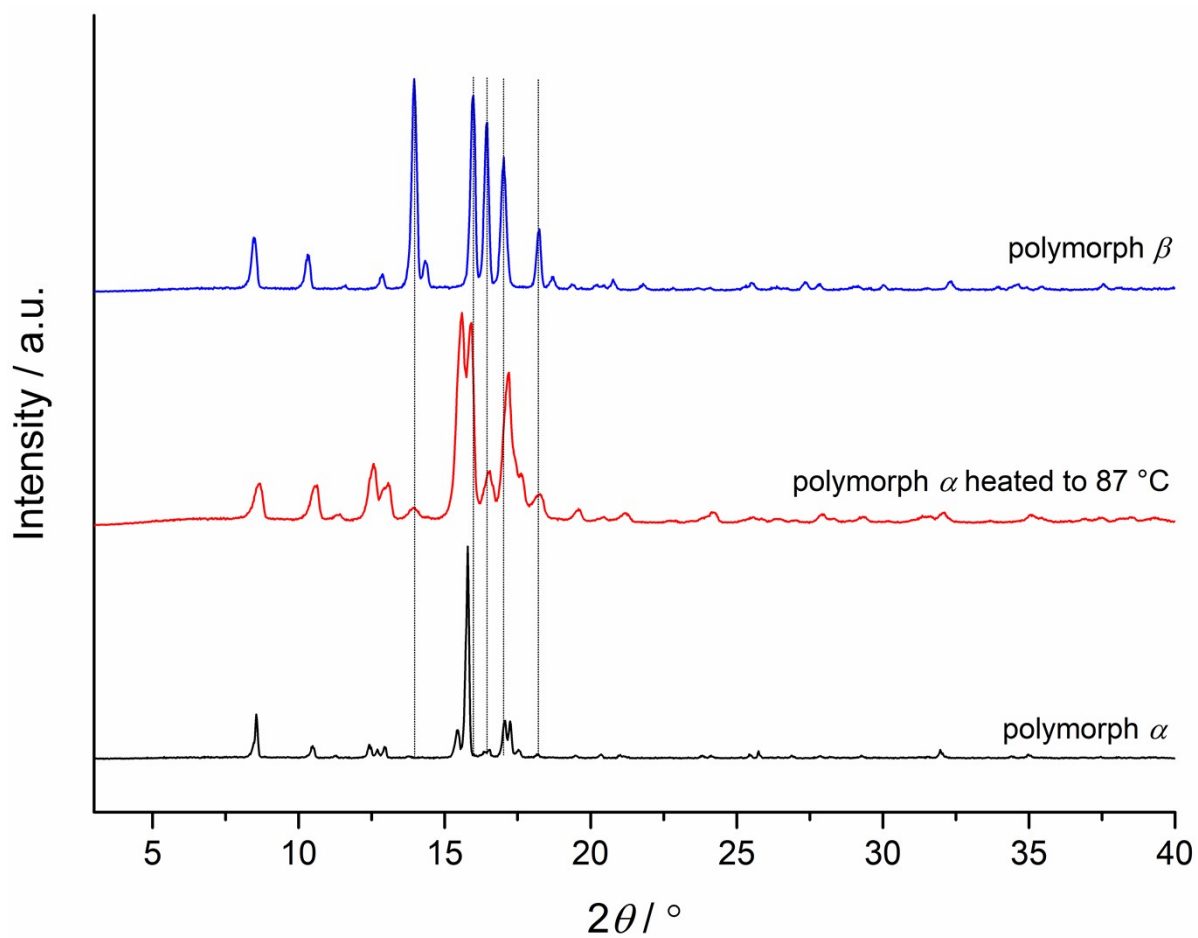


Fig. S10. PXRD patterns showing the mixture of polymorphs after heating and milling polymorph α to 87 °C ($\lambda = 1.54 \text{ \AA}$).

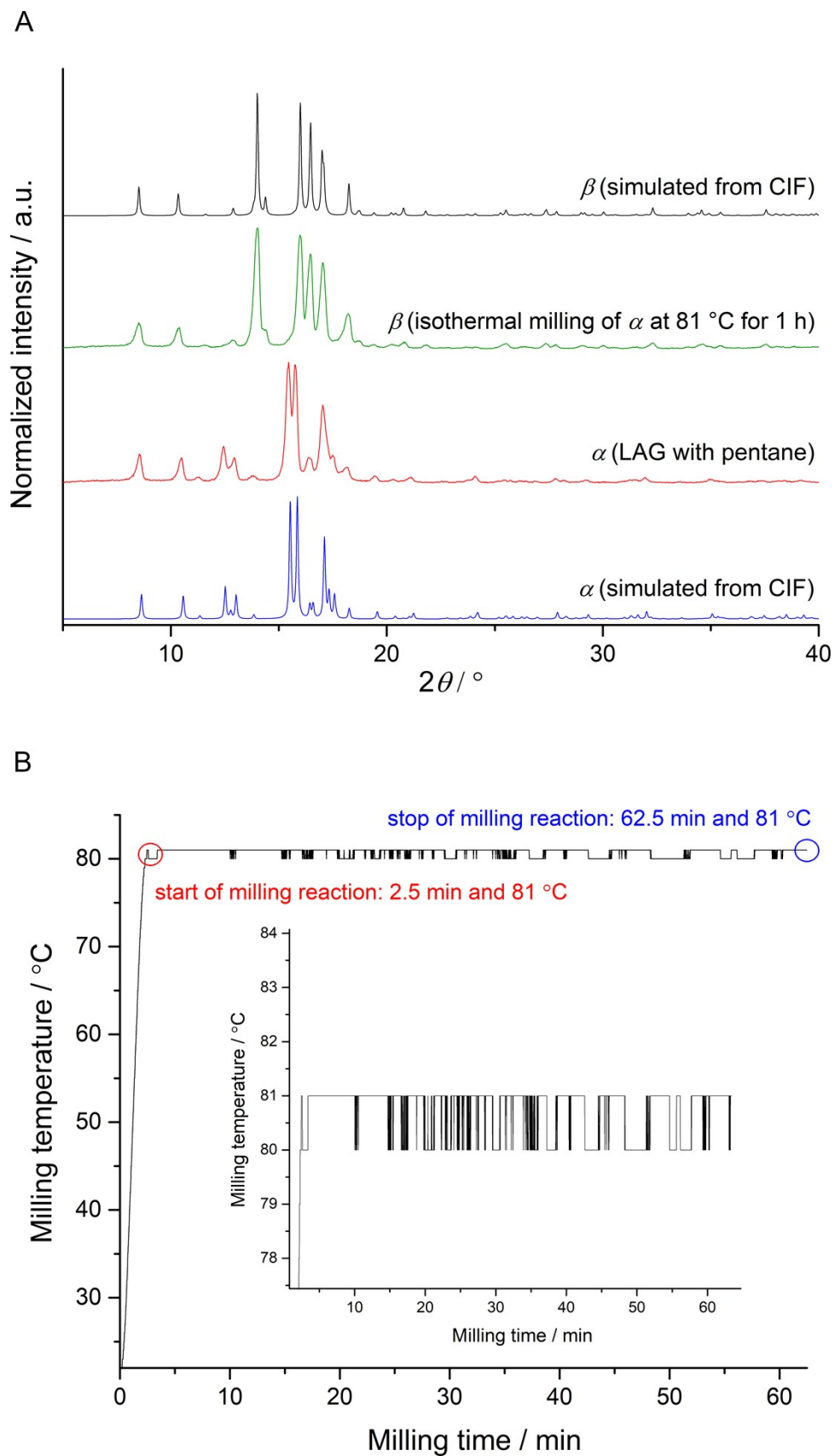


Fig. S11. A) PXRD patterns showing that polymorph β formed after isothermal milling of polymorph α at 81 °C for 1 h ($\lambda = 1.54 \text{ \AA}$). B) Time-resolved in situ monitoring of milling temperature corresponding to conditions in A). The inset shows detailed variation of milling temperature between 80 and 81°C.

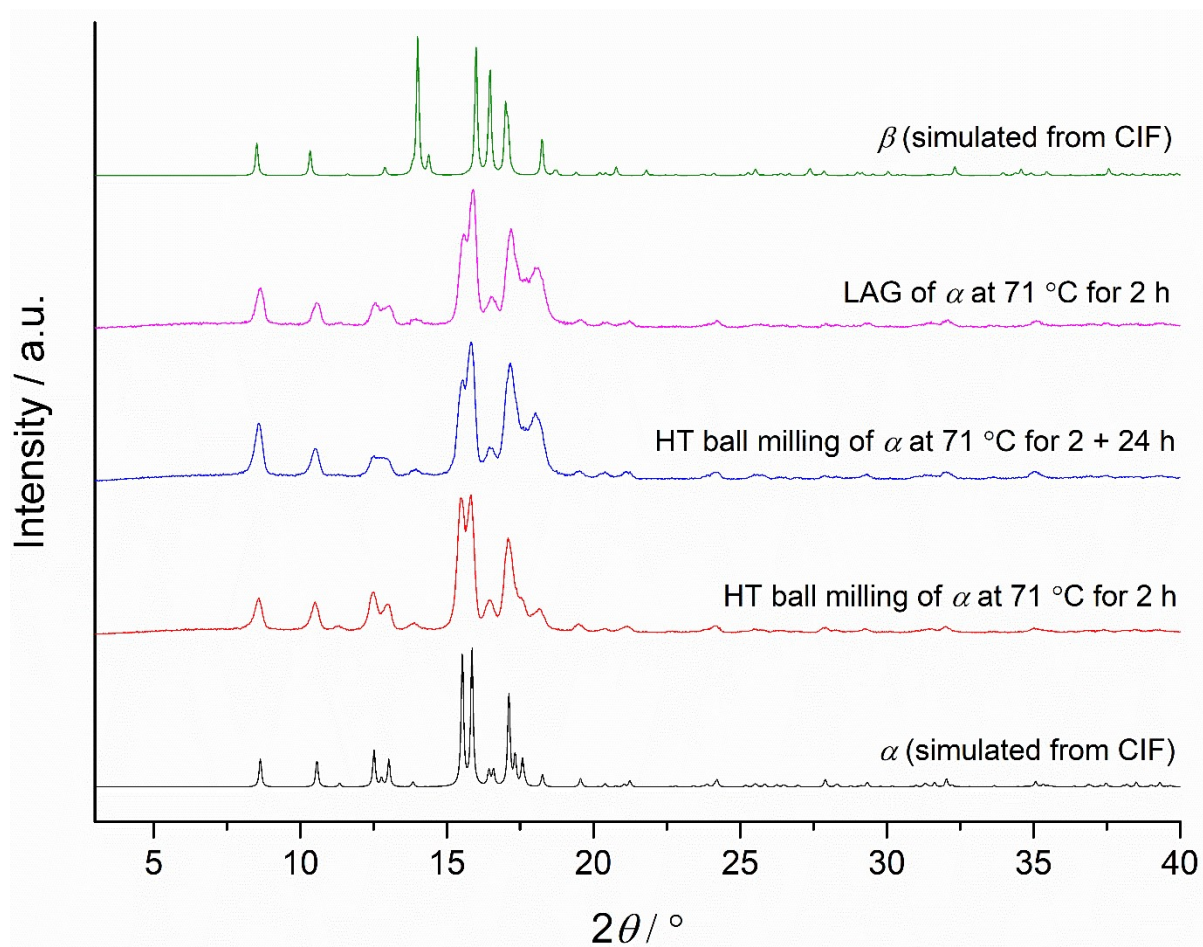


Fig. S12. PXRD patterns showing the results of isothermal milling of polymorph α at different milling conditions ($\lambda = 1.54 \text{ \AA}$).

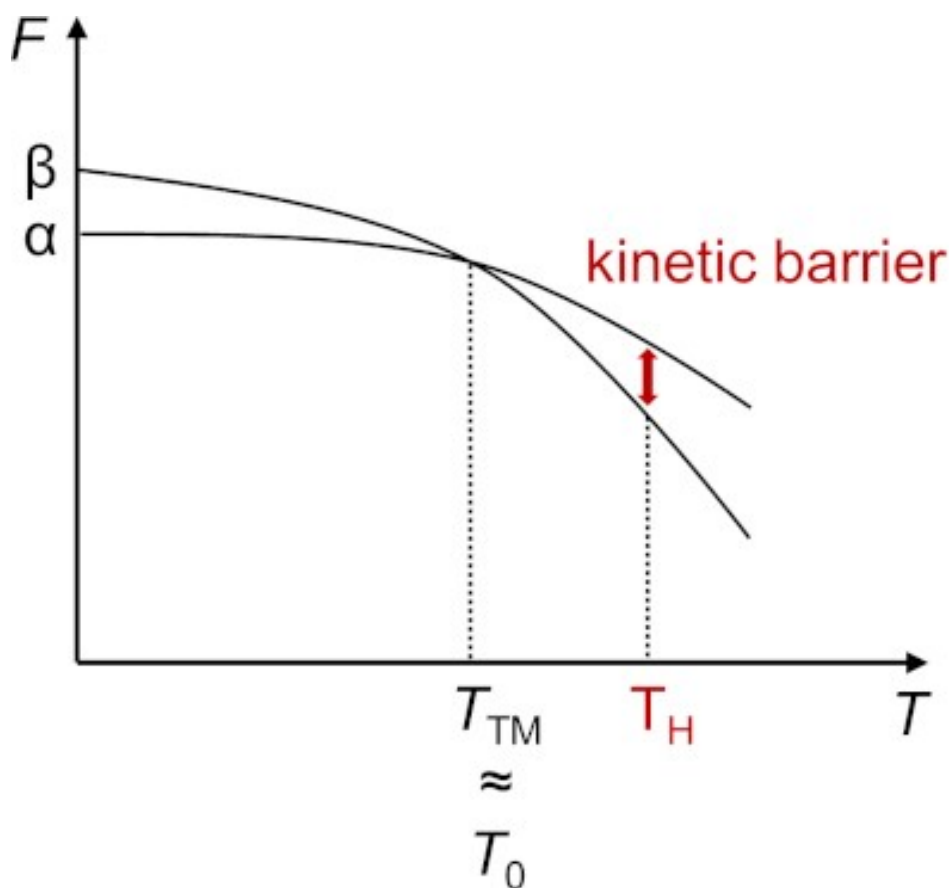


Fig. S13. The concept of different temperatures of phase transitions when heating and thermo-milling and how milling can overcome the kinetic barrier that is associated with phase transition. $\Delta T = T_H - T_0$; $T_0 \approx T_M$, where T_H is the DSC transition temperature, T_M is the thermo-mechanochemical transition temperature, and T_0 is the thermodynamical transition temperature at which free energies of the two polymorphs are the same.

References

- 1) J. Alić, T. Stolar, Z. Štefanić, K. Užarević and M. Šekutor, *ACS Sustain. Chem. Eng.*, 2023, **11**, 617.
- 2) N. Cindro, M. Tireli, B. Karadeniz, T. Mrla and K. Užarević, *ACS Sustainable Chem. Eng.*, 2019, **7**, 16301.
- 3) <https://assets.omega.com/manuals/M5461.pdf>
- 4) E. J. Sonneveld and J. W. Visser, *J. Appl. Crystallogr.*, 1975, **8**, 1.
- 5) O. V. Dolomanov, L. J. Bourhis, R. J. Gildea, J. A. K. Howard and H. Puschmann, *J. Appl. Crystallogr.*, 2009, **42**, 339.
- 6) G. Sheldrick, *Acta Crystallogr. Sect. A*, 2015, **71**, 3.
- 7) J. P. Perdew, K. Burke and M. Ernzerhof, *Phys. Rev. Lett.*, 1996, **77**, 3865.
- 8) A. Ambrosetti, A. M. Reilly, R. A. DiStasio Jr. and A. Tkachenko, *J. Chem. Phys.*, 2014, **140**, 18A508.

- 9) V. Blum, R. Gehrke, F. Hanke, P. Havu, V. Havu, X. Ren, K. Reuter and M. Scheffler, *Comput. Phys. Commun.*, 2009, **180**, 2175.
- 10) J. Hermann, M. Stöhr, S. Góger, S. Chaudhuri, B. Aradi, R. J. Maurer and A. Tkatchenko, *J. Chem. Phys.*, 2023, **159**, 174802.
- 11) C. Devereux, J. S. Smith, K. K. Huddleston, K. Barros, R. Zubatyuk, O. Isayev and A. E. Roitberg, *J. Chem. Theory Comput.*, 2020, **16**, 4192.
- 12) X. Gao, F. Ramezanghorbani, O. Isayev, J. S. Smith and A. E. Roitberg, *J. Chem. Inf. Model.*, 2020, **60**, 3408.
- 13) E. Caldeweyher, J.-M. Mewes, S. Ehlerta and S. Grimme, *Phys. Chem. Chem. Phys.*, 2020, **22**, 8499.
- 14) A. H. Larsen *et al.*, *J. Phys.: Condens. Matter*, 2017, **29**, 273002.
- 15) A. Togo *et al.*, *J. Phys.: Condens. Matter*, 2023, **35**, 353001.
- 16) A. Togo, *J. Phys. Soc. Jpn.*, 2023, **92**, 012001.